

## Interference Test Analysis Using Linear Flow Model A Case Study

K. C. Fan, M. C. Tom Kuo\*, K. F. Liang, S. C. Chiang

Department of Mineral and Petroleum Engineering, National Cheng Kung University, Tainan, Taiwan

\* Fax: 886-6-2747378. E-mail address: [mctkuobe@mail.ncku.edu.tw](mailto:mctkuobe@mail.ncku.edu.tw) (M. C. Tom Kuo).

**Keywords:** Reservoir, well tests, thermal water, Chingshui, Taiwan.

### ABSTRACT

Thermal water production in Chingshui geothermal reservoir is largely from the fracture zone in the Jentse member of Lushan Formation, which is evidently controlled by the predominant joints and active faults. Because the rock matrix has very low permeability, the fracture system provides the main conduit for fluid flow. Linear flow appears to be a more likely configuration than radial flow.

A conceptual linear flow model was developed based on geological data of Chingshui geothermal area. Field data of interference test in Chingshui geothermal field appears to be rare in the literature. Linear flow models were used to analyze an interference test in Chingshui geothermal reservoir to determine values of reservoir transmissivity and porosity-thickness product.

### 1. INTRODUCTION

The Chingshui geothermal field is located in the northeast portion of Taiwan. An interference test was conducted for the initial assessment of Chingshui geothermal reservoir. The main objective was to determine the transmissivity and coefficient of storage for estimating deliverability and reserves, respectively.

Subsurface data indicate that thermal water production in Chingshui geothermal field is largely from the fracture zone in the steeply dipping Jentse Member (Hsiao and Chiang, 1979). Predominant joints are well developed in the Jentse Member. Structural analysis shows that the strike of steeply dipping predominant joints is between N 25° W and N 40° W.

Conventional interference analysis based on the line source solution relies on the assumption that flow to the production well is predominantly radial. In a fractured

geothermal reservoir, the flow is largely through fractures in the effectively impermeable rock matrix. For radial flow to occur, the orientations of the fractures must be randomly distributed in all directions.

The outcrop nearby Chingshui thermal manifest area also shows faults run parallel for almost 100 to 150 meters striking in the direction between N 30° W and N 35° W (Tseng, 1978).

All the wells at the depth of the production interval are deviated almost parallel to the joints existing at the surface (Hsiao and Chiang, 1979).

For this apparent linear trend of the fractures in the production zone, it appears more appropriate to represent

the flow between wells by a linear flow model than a radial flow model.

A conceptual linear flow model was developed based on geological data of Chingshui geothermal area including stratigraphy, structure, hydrothermal system, and fracture system. The Miller solution based on linear flow, was used to analyze the well interference test and to determine values of reservoir transmissivity and porosity-thickness product.

### 2. GEOLOGY

The Chingshui geothermal area is an area of hot springs situated along Chingshui River, approximately 13 km southwest of Lotung, Taiwan, as shown in Figure 1. Geologically, this area is composed of dark-gray and black slates, namely the Miocene Lushan Formation. Lushan Formation can be lithologically divided into three members: the Jentse Member, the Chingshuihu Member, and the Kulu Member. Generally, the Jentse Member is mainly composed of metasandstone intercalated in slate, while the underlying Chingshuihu Member and Kulu Member consist mostly of slate (Tseng, 1978; Chiang et al., 1979).

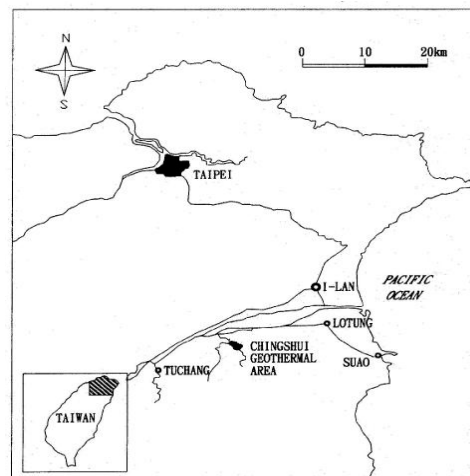


**Figure 1: Location map of the Chingshui geothermal area.**

The monocline structure is cut internally by numerous thrust faults, trending principally parallel to the bedding (NE-SW) and slightly curved. These are: the Tashi fault, the Hsiaonanao fault, and the Hanhsia fault, as shown in Figure 2 (Su, 1978; Hsiao and Chiang, 1979). Along Chingshui River, there is a normal fault, the Chingshuihsia fault, which trends N-S in the Chingshui geothermal field situated on the monocline. The most convex of the NE-SW faults exists around the Chingshui geothermal field. It is postulated that the shear folding tectonic movements might have occurred with a greater tensile stress around the

Chingshui geothermal field, which would cause fractures in the slate to be well developed. Jentse, and Kulu members of the Miocene Lushan Formation.

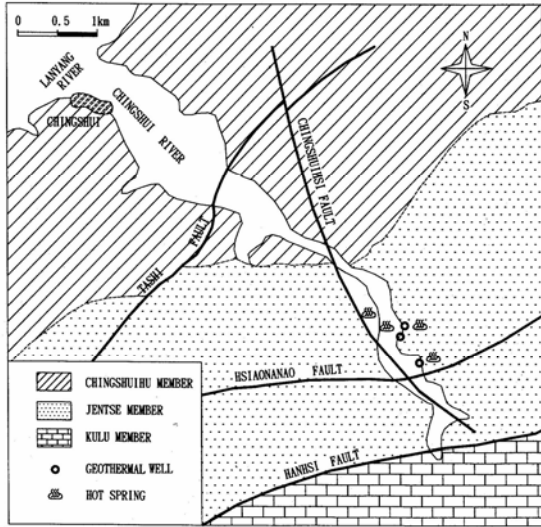


**Figure 2: Geological map of the Chingshui geothermal area showing Chingshuihu, Jentse, and Kulu members of the Miocene Lushan Formation.**

Sufficient available data indicate that thermal fluid reservoir is formed by fractures. Due to the poor porosity and permeability of the slate rock, faults, joints, and other extensive fractures provide conduits of geothermal water production. Predominant joints, which are almost aligned perpendicular to the strike of the strata, are found densely developed in the sandy Jentse Member.

Figure 3 shows the Rose diagram of 67 joints measured from the outcrop of the sandy Jentse Member nearby the Chingshui geothermal field (Tseng, 1978). The most prominent set of joints strikes northwest and dips between  $65^0$  and  $80^0$  to the southwest. A less conspicuous set strikes northeast and dips steeply northwest.

In addition, the Chingshui River almost trends parallel to the joints. It is formed by erosion of the slate outcrops with well-developed fractures. There are numerous hot springs and fumaroles along the sides of the running river in the Chingshui geothermal field. It is reasonable to interpret that the riverbed is the area where the major open fractures reach the surface.

The geothermal reservoirs consist of well-developed joints or faults. All the wells drilled in the Jentse Member are inclined with a rather high angle up to  $35^0$ , and all are deviated almost parallel to the joints existing at the surface. Furthermore, some wells changed their deviations abruptly and turned back in direction sharply almost parallel to the joints with a loss of mud circulation when a highly productive fractured zone was encountered.

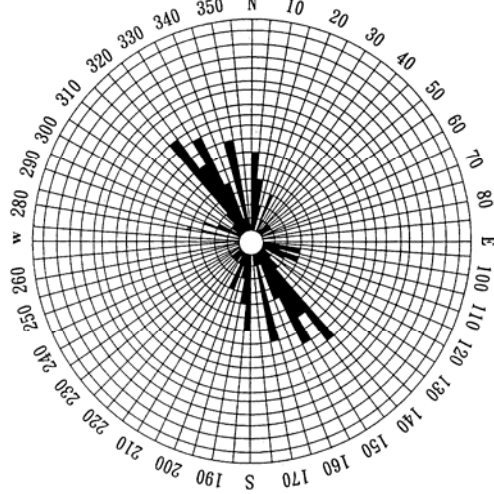


**Figure 3: Rose diagram of 67 joints in the Chingshui geothermal area (Tseng, 1978).**

### 3. Well completion and capacity

Bentonite slurry treated with chrome lignosulfonate chemical was used for drilling circulation. For preventing the hole from caving, the mud always maintained proper properties with a weight of 1.10 to 1.25 in specific gravity and 40 seconds in Marsh funnel viscosity. Heavy loss of circulation has occurred when a major fracture zone has been penetrated during drilling. Fresh water was finally injected into the well to replace the mud for well completion.

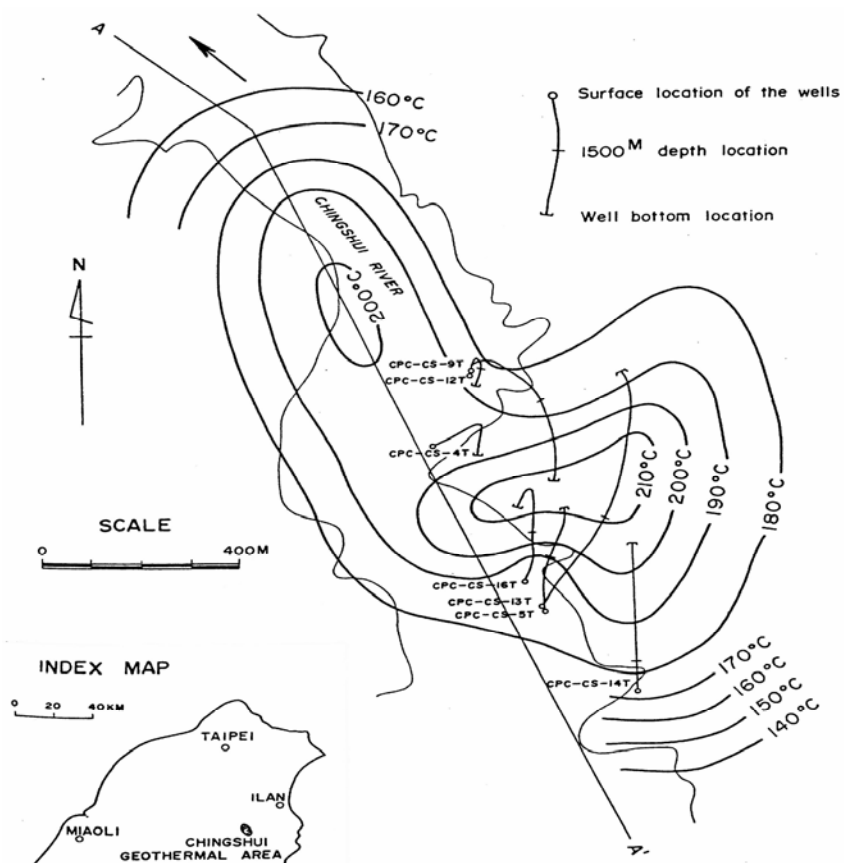
The casing program of the production wells is 50.8 cm (20 in.) conductor, 34 cm (13-3/8 in.) surface casing, 24.4 cm (9-5/8 in.) production casing, and 17.8 cm (7 in.) or 11.4 cm (4-1/2 in.) slotted liner. The depth of the slotted liner hanger varied from 490 to 1048 m, depending upon the depth of the high temperature production zone, while the length of the liner for each well varied from 950 to 2160 m. Cementing has been done for the conductor, surface, and production casings. Table 1 summarizes the completion and capacity data for all the production wells, 4T, 5T, 9T, 12T, 13T, 14T, and 16T. The well capacity was measured with James method (1966) by discharging steam-water mixtures at the speed of sound to the atmosphere.

### 4. INTERFERENCE TEST

An interference test was conducted during November of 1979 (Chang and Ramey, 1979). During this test, Well 16T was produced, and pressure responses were observed in Wells 4T, 5T, 9T, 12T, 13T, and 14T. Figure 4 is a scale map showing both surface and bottom-hole locations of these wells. Because all wells were drilled, it was necessary to estimate distance between the bottom-hole locations for interpretation of interference tests. The results of the interference test are presented in Table 2. As can be seen, the production rate of weir hot water ranged from 80 to 84 tons/hour during the eleven-day interference test. The test was conducted by observing wellhead pressures at the observation wells. A complete set of interference data is presented in Table 2 because field data appears to be rare in the literature. The interference data for Wells 5T and 13T do not appear to be reliable because of some malfunction of equipment. The theory and interpretation of the interference test results will be presented as follows.

**Table 1. Well capacity and completion data for wells in Chingshui geothermal reservoir**

Well number	Elevation (m)	Well capacity			Well completion			
		Steam rate (tons/hr)	Hot water rate (tons/hr)	Total flow rate (tons/hr)	Total depth, TD. (m)	Shoe of liner (m)	Liner hanger (m)	Temperature at TD, (°C)
4T	257.95	28.6	98.1	126.7	1505	1503	498	201
5T	269.54	6	34	40	2005	1998	493	220
9T	260.67	18.7	55.3	74	2079	2074	490	205
12T	260.67	6.9	40	46.9	2003	1998	1048	223
13T	269.54	10.44	60.14	70.58	2020	2015	505	219
14T	281.50	22	66	88	2003	1995	947	215
16T	272.58	30.3	85.9	116.2	3000	2990	830	225

**Figure 4: Location of the wells and the isotherms of presumed formation temperature for 1500 m depth in the Chingshui geothermal area (Chang and Ramey, 1979).**

**Table 2. Interference test in Chingshui geothermal field (Chang and Ramey, 1979)**

Time	Observation wells												Flowing Well				
	4T				9T				12T				14T				16T
	WHP <sup>§</sup>	kg/cm <sup>2</sup>	psi	Δp **	WHP	kg/cm <sup>2</sup>	psi	Δp	WHP	kg/cm <sup>2</sup>	psi	Δp	WHP	kg/cm <sup>2</sup>	psi	Flow Rate	tons/hr
ht																	
12.09	172	0.00	C		9.70	138	0.00	C	13.15	187	0.00	C	9.35	133	0.00	18.14	258
12.02	171	0.07	1		9.63	137	0.07	1	13.01	185	0.14	2	9.35	133	0.00	4.85	69
11.81	168	0.28	4		9.49	135	0.21	3	11.39	162	0.35	5	9.14	130	0.21	4.08	58
11.67	166	0.42	€		9.35	133	0.35	5	12.80	182	0.35	5	8.79	125	0.56	3.94	56
11.67	166	0.42	€		9.14	130	0.56	8	12.66	180	0.49	7	8.79	125	0.56	3.94	56
11.66	165	0.49	7		9.14	130	0.56	8	12.59	179	0.56	8	8.65	123	0.70	3.94	56
11.53	164	0.56	8		9.14	130	0.56	8	12.52	178	0.63	9	8.51	121	0.84	3.94	56
11.53	164	0.56	8		9.07	129	0.63	9	12.44	177	0.70	10	8.44	120	0.91	3.80	54
11.46	163	0.63	9		9.00	128	0.70	10	12.37	176	0.77	11	8.37	119	0.98	3.80	54
11.39	162	0.70	10		8.93	127	0.77	11	12.30	175	0.84	12	8.37	119	1.05	3.73	53
11.39	162	0.70	10		8.93	127	0.77	11	12.30	175	0.84	12	8.23	117	1.12	3.66	52
11.32	161	0.77	11		8.86	126	0.84	12	12.30	175	0.84	12	8.09	115	1.27	3.66	52
																80**	

\* WHP: Wellhead pressure.

\*\*: Pressure interference.

\*\*\* Equivalent of well stream total production rate of 105 tons/hr.

## 5. LINEAR FLOW MODEL

A conceptual linear flow model was developed based on geological data of Chingshui geothermal area including stratigraphy, structure, hydrothermal system, and fracture system. Figure 5 shows a schematic drawing of the linear flow model for Chingshui geothermal reservoir. All the wells drilled in Chingshui geothermal reservoir intercepted fracture planes.

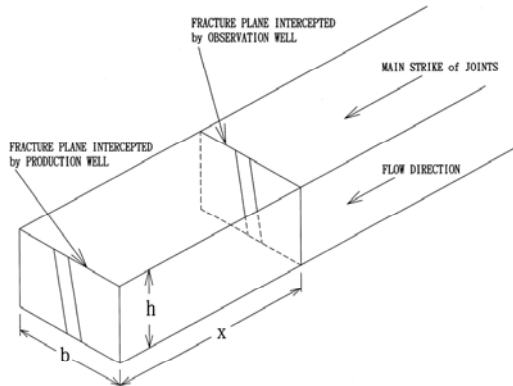


**Figure 5: Schematic drawing of a linear flow model for a fractured reservoir.**

Chingshui geothermal reservoir is represented by a parallelepiped. Fluid flow is parallel to the main strike of joints and the lateral boundaries of the parallelepiped. The cross-section of the parallelepiped is assumed to be a rectangle with height  $h$  and width  $b$ . The production well is represented by a planar source. The diffusivity equation governing fluid flow in an infinite reservoir for the constant-rate case may be stated as follows.

$$\frac{\partial p}{\partial t} = a \frac{\partial^2 p}{\partial x^2} \quad (1)$$

is the subject to the following initial and boundary conditions:

$$t = 0, \quad p = p_i \quad \text{for } x \geq 0$$

and

$$t > 0, \quad \frac{\partial p}{\partial x} = \frac{q\mu}{bhk} \quad \text{for } x = 0 \quad \text{and}$$

$$\lim_{x \rightarrow \infty} p(x, t) = p_i \quad \text{for } x \rightarrow \infty$$

where  $a = k/\phi\mu c_t$  is the formation diffusivity.

Miller (1960) investigated unsteady influx of water in linear reservoirs for the constant-rate case and an infinite-acting reservoir with the same equations as above. Miller developed the following solution.

$$p(x, t) = p_i - \frac{q\mu}{khb} \left[ 2\sqrt{\frac{at}{\pi}} \exp\left(-\frac{x^2}{4at}\right) - x \operatorname{erfc}\left(\frac{x}{2\sqrt{at}}\right) \right] \quad (2)$$

Miller's solution, Equation (2), is similar to the solution developed by Jenkins and Prentice (1982) for aquifer test analysis in fractured rocks under linear flow conditions. The Miller solution was applied to a steam reservoir for interference analysis (Ehlig-Economides et al., 1980). To apply Miller's solution to a fractured hot-water reservoir, the following dimensionless variables are first defined in metric units.

$$P_{Dl} = \frac{kh\Delta p}{0.4568 (2\pi) v_{sc} q\mu B} \quad (3)$$

$$x_D = x/b \quad (4)$$

$$t_{Db} = \frac{0.3604 kht}{\phi h \mu c_t b^2} \quad (5)$$

where  $x$  is distance between the production and observation well, m; and  $b$  is width of the fractured reservoir, m. Then, Equation (2) can be written in terms of dimensionless variables defined above.

$$\frac{P_{Dl}}{x_D} = 2 \sqrt{\frac{t_{Db}}{\pi x_D^2}} \exp\left(-\frac{x_D^2}{4t_{Db}}\right) - \operatorname{erfc}\left(\frac{x_D}{2\sqrt{t_{Db}}}\right) \quad (6)$$

Equation (6) can be used to calculate a log-log type-curve,  $P_{Dl}/x_D$  versus  $t_{Db}/x_D^2$  for linear flow. For the purpose of interference analysis, it is assumed that half of the produced fluid comes from both sides of production well. Figure 5 shows only one side for a production well along the direction of fluid flow and the main strike of joints.

## 6. INTERPRETATION OF INTERFERENCE TEST RESULTS

The interpretation of the interference test results by log-log type-curve matching will be presented for Well 4T. Figure 6 is a match of the pressure versus time data of Well 4T with Miller solution for linear flow.

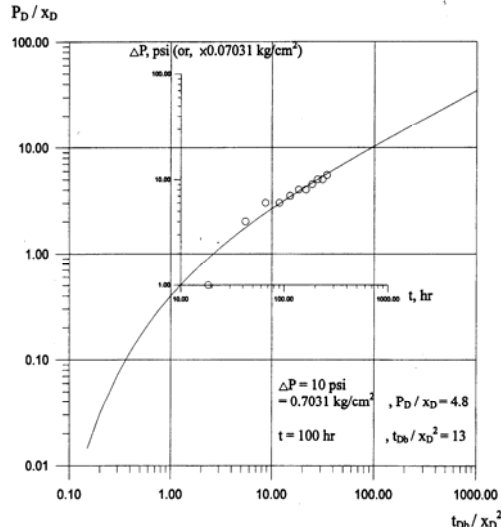


Figure 6: Type-curve match for well 4T using linear flow model.

The following match points can be obtained for Well 4T:

$$P_{Dl}/x_D = 48 \quad \Delta P = 0.7031 \text{ kg/cm}^2 \text{ (or, } 10 \text{ psi)}$$

$$t_{Db}/x_D^2 = 13 \quad t = 100 \text{ hr}$$

Given the following data:

$$q = (0.5)(105) \text{ tons/hr}$$

$$v_{sc} = 1.08 \text{ cm}^3/\text{g}$$

$$x = 175 \text{ m}$$

$$b = 300 \text{ m}$$

Using Equation (3) and (4), and solving for the  $kh$  product:

$$\frac{P_{Dl}}{x_D} = \frac{kh\Delta pb}{0.4568 (2\pi)v_{sc} q\mu Bx}$$

$$4.8 = \frac{kh(0.7031)(300)}{0.4568(2\pi)(1.08)(0.5)(105)(0.12)(1.1)(175)}$$

$$kh = 85.5 \text{ Darcy-meter}$$

Using Equation (4) and (5), and solving for the  $\phi h$  product:

$$\frac{t_{Db}}{x_D^2} = \frac{0.3604 kht}{\phi h \mu c_i x^2}$$

$$13 = \frac{(0.3604)(85.5)(100)}{\phi h(0.12)(1.42 \times 10^{-4})(175)^2}$$

$$\phi h = 452 \text{ m}$$

Figure 7 shows the match of the pressure versus time data of Well 9T with the Miller solution. The data for Well 12T and Well 14T also are shown on Figure 8 and Figure 9. Table 3 summarizes the results of type-curve matching for all the well pairs during this test using linear flow model. As can be seen in Table 3, porosity-thickness for all the well pairs was reasonably similar in the range of 270 to 924 m. Most importantly, permeability-thickness for each well pair appeared to correlate decently with well capacity observed in production tests.

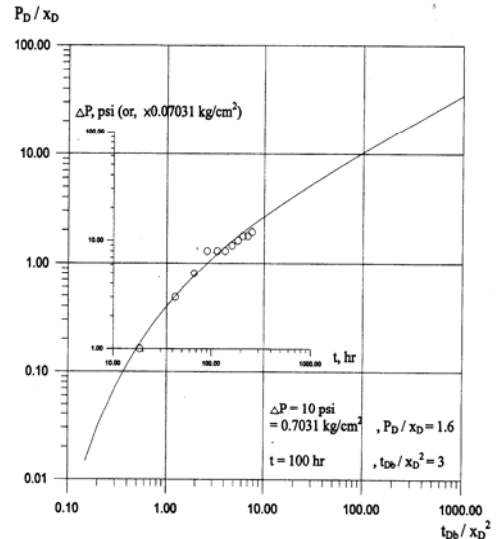


Figure 7: Type-curve match for well 9T using linear flow model.

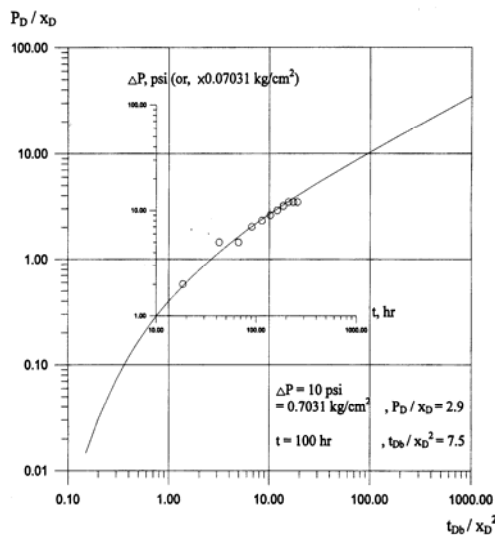


Figure 8: Type-curve match for well 12T using linear flow model.

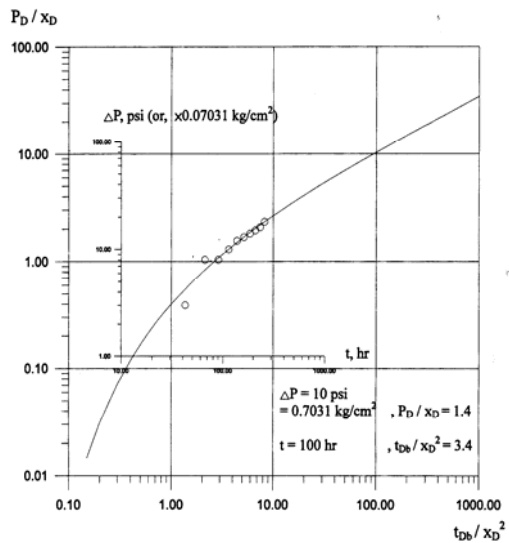


Figure 9: Type-curve match for well 14T using linear flow model.

Table 3. Type curve matching using Miller solution

Linear flow model	Observation wells				Average $\pm$ Std. Dev.
	4T	9T	12T	14T	
Match point					
$\Delta P = 0.7031 \text{ kg/cm}^2, P_D / x_D = 4.8$ ( $\Delta P = 10 \text{ psi}$ )	4.8	1.6	2.9	1.4	
$t = 100 \text{ hrs}, t_Db / x_D^2 = 13$	13	3	7.5	3.4	
Distance, m	175	300	90	330	
$kh$ , Darcy-meter	85.5	48.9	26.6	47.1	$52.0 \pm 24.5$
$\phi h$ , m	452	383	924	270	$507 \pm 288$

## 7. CONCLUSIONS

A method using a linear flow model for interpreting interference test in fractured reservoir was presented in this paper. Miller solution can be used for linear flow configuration. To apply Miller solution for analyzing interference test correctly, a conceptual linear flow model must first be developed based on geology.

The geological data of Chingshui geothermal area including stratigraphy, structure, and fracture system strongly support the use of a linear flow model for interference-test analysis. The interference-test analysis shows that the data can be matched to the type curves of linear flow models. When the values of permeability-thickness product determined from the model matches are correlated with the well productivities, the linear flow model was excellent.

The linear flow model developed was found not only valid for interference analysis but also instrumental for reserves estimation of Chingshui geothermal field. Porosity-thickness product is a key parameter used in the volumetric calculation of the fluid-in-place of geothermal reservoirs.

## ACKNOWLEDGMENTS

This research was funded by the Energy Commission, Ministry of Economic Affairs and National Science Council of Taiwan (NSC-92-ET-7-006-002-ET and NSC-93-2623-7-006-006-ET).

## REFERENCES

Chang, C. R. Y., Ramey, H. J.: Well interference test in the Chingshui geothermal field. *Proceedings, 5th Workshop on Geothermal Reservoir Engineering*, Stanford University, Stanford, CA(1979).

Chiang, S. C., Lin, J. J., Chang, C. R. Y., Wu, T. M.: A preliminary study of the Chingshui geothermal area, Ilan, Taiwan. *Proceedings, 5th Workshop on Geothermal Reservoir Engineering*, Stanford University, Stanford, CA(1977).

Earlougher, R. C.: Advances in well test analysis. Monograph Series 5, Society of Petroleum Engineers of AIME, Dallas.

Ehlig-Economides, Economides, C., M. J., Miller, F. G.: Interference between wells in a fractured formation, *Geothermal Resources Council, Transactions* 4, (1980), 321-324.

Hsiao, P. T., Chiang, S. C.: Geology and geothermal system of the Chingshui-Tuchang geothermal area, Ilan, Taiwan, *Petroleum Geology of Taiwan*, **16**, (1979), 205-213.

James, R.: Measurement of steam-water mixtures at the speed of sound to the atmosphere, *New Zealand Engineering*, **20** (1), (1966), 437-441.

Jenkins, D. N., Prentice, J. K.: Theory for aquifer test analysis in fractured rocks under linear (nonradial) flow conditions, *Ground Water*, **20** (1), (1982), 12-21.

Kuo, M. C. T., Wang, W. L., Lin, D. S., Lin, C. C., Chiang, C. J.: An image-well method for predicting drawdown distribution in aquifers with irregularly shaped boundaries, *Ground Water*, **32** (5), (1994), 794-804.

Lang, S. M.: Interpretation of boundary effects from pumping test data, *American Water Works Association Journal*, **52** (3), (1960), 356-364.

Miller, F. G.: Theory of unsteady-state influx of water in linear reservoirs, Report, **45** pp., Stanford University, Stanford, CA(1960).

Papadopoulos, I. S.: Nonsteady flow to a well in an infinite anisotropic aquifer. Symposium International Assn. Sci. Hydrology, Dubrovnik, Yugoslavia(1965).

Ramey, H. J.: Interference analysis for anisotropic formations-a case history, *Journal of Petroleum Technology*, (1975), 1290-1298.

Su, F. C.: Resistivity survey in the Chingshui prospect, Ilan, Taiwan, *Petroleum Geology of Taiwan*, **15**, (1978), 255-264.

Tseng, C. S.: Geology and geothermal occurrence of the Chingshui and Tuchang districts, Ilan, *Petroleum Geology of Taiwan* **15**, (1978), 11-23.